AMERICAN SOCIETY FOR MICROBIOLOGY | Applied and Environmental Microbiology®

PHYSIOLOGY

Human Urine Alters Methicillin-Resistant *Staphylococcus aureus* Virulence and Transcriptome

Santosh Paudel,[a] Kamal Bagale,[a] Swapnil Patel,[a] Nicholas J. Kooyers,[a] Ritwij Kulkarni[a]

[a]Department of Biology, University of Louisiana at Lafayette, Lafayette, Louisiana, USA

Santosh Paudel and Kamal Bagale contributed equally to this work. Author order was determined randomly.

ABSTRACT Gram-positive methicillin-resistant *Staphylococcus aureus* (MRSA) is an emerging cause of hospital-associated urinary tract infections (UTI), especially in catheterized individuals. Despite being rare, MRSA UTI are prone to potentially life-threatening exacerbations such as bacteremia that can be refractory to routine antibiotic therapy. To delineate the molecular mechanisms governing MRSA urinary pathogenesis, we exposed three *S. aureus* clinical isolates, including two MRSA strains, to human urine for 2 h and analyzed virulence characteristics and changes in gene expression. The *in vitro* virulence assays showed that human urine rapidly alters adherence to human bladder epithelial cells and fibronectin, hemolysis of sheep red blood cells (RBCs), and surface hydrophobicity in a staphylococcal strain-specific manner. In addition, transcriptome sequencing (RNA-Seq) analysis of uropathogenic strain MRSA-1369 revealed that 2-h-long exposure to human urine alters MRSA transcriptome by modifying expression of genes encoding enzymes catalyzing metabolic pathways, virulence factors, and transcriptional regulators. In summary, our results provide important insights into how human urine specifically and rapidly alters MRSA physiology and facilitates MRSA survival in the nutrient-limiting and hostile urinary microenvironment.

IMPORTANCE Methicillin-resistant *Staphylococcus aureus* (MRSA) is an uncommon cause of urinary tract infections (UTI) in the general population. However, it is important to understand MRSA pathophysiology in the urinary tract because isolation of MRSA in urine samples often precedes potentially life-threatening MRSA bacteremia. In this report, we describe how exposure to human urine alters MRSA global gene expression and virulence. We hypothesize that these alterations may aid MRSA in acclimating to the nutrient-limiting, immunologically hostile conditions within the urinary tract leading to MRSA UTI.

KEYWORDS MRSA, RNA-Seq, *Staphylococcus aureus*, UTI, transcriptome analysis, urinary tract infection, virulence

Gram-positive pathogen *Staphylococcus aureus* is an emerging cause of urinary tract infections (UTI) representing 1% of uncomplicated cases and 3% of complicated cases associated with the physical obstruction of the urinary tract (1). Urinary catheterization is the single most important predisposing factor for persistent *S. aureus* colonization of the urinary tract that substantially increases the risk of symptomatic UTI and potentially life-threatening, invasive sequelae such as bacteremia, endocarditis, and septic shock (2–4). In addition, up to 20% of *S. aureus* catheter-associated UTI (CAUTI) are caused by methicillin-resistant *S. aureus* (MRSA), which are resistant to routine antibiotic therapy (5). Hence, defining the complex interactions between host immune defenses and pathogen virulence effectors during the course of MRSA UTI is a clinically relevant research area despite relatively low prevalence of MRSA UTI.

Citation Paudel S, Bagale K, Patel S, Kooyers NJ, Kulkarni R. 2021. Human urine alters methicillin-resistant *Staphylococcus aureus* virulence and transcriptome. Appl Environ Microbiol 87:e00744-21. https://doi.org/10.1128/AEM.00744-21.

Editor Charles M. Dozois, INRS—Institut Armand-Frappier

Address correspondence to Ritwij Kulkarni, ritwij.kulkarni@louisiana.edu.

Received 19 April 2021
Accepted 3 June 2021
Accepted manuscript posted online 9 June 2021
Published 27 July 2021

Previous experiments have identified bacterial virulence factors central to the urinary pathogenesis of *S. aureus*. Examination of *S. aureus* isolated from catheterized patients has revealed that ~80% of the clinical isolates form biofilm, a virulence characteristic associated with the presence of *icaA* and *icaD* genes encoding polysaccharide capsule (6). The trace metal nickel/cobalt transporter systems are implicated in the urinary fitness and virulence of *S. aureus* due to the involvement of nickel as a cofactor in urease enzyme activity (7, 8). MRSA infection is shown to exacerbate catheterization-induced bladder inflammation in a mouse model by inducing prolonged production of potent pro-inflammatory cytokines (interleukin 1-alpha [IL-1α], IL-1β, IL-6, IL-17, and tumor necrosis factor alpha [TNF-α]) and the recruitment of macrophages and neutrophils (9). It has also been observed that MRSA facilitates bladder colonization by inducing accumulation of host protein fibrinogen on urinary catheters, to which it adheres via surface adhesins, clumping factors A and B (ClfA, ClfB) (9). Collectively, these studies have identified virulence factors that afford survival advantage to MRSA inside the urinary tract and immune responses that defend the host. However, these studies were not designed to define the pleiotropic effects of urinary microenvironment on MRSA physiology, which is the main objective of our project.

To delineate complex mechanisms regulating the survival of uropathogens in the human urinary tract and their ability to cause UTI, the ideal experimental setup would be to examine bacterial transcriptome and proteome in real time through different stages of UTI in a human host. Given the obvious impracticability of this setup, we explored a more practical alternative and analyzed MRSA physiology in human urine (HU) *in vitro*. We used three *S. aureus* strains, including MRSA-1369 and PUTS-1, which are clinical isolates from urine (9), and USA300, which has emerged in the last 2 decades as the predominant community-associated MRSA strain in the United States (10). We used *in vitro* virulence assays to compare these strains exposed to HU with control in nutrient-rich culture medium. In addition, we used RNA sequencing (RNA-Seq) to compare global transcriptomic profiles of MRSA-1369 exposed for 2 h to HU or nutrient-rich tryptic soy broth (TSB). Our results reveal that in addition to myriad metabolic adaptations necessary for survival in nutrient-limiting conditions in urine, staphylococci in human urine also exhibit changes in virulence characteristics such as adherence to uroepithelial cells and extracellular matrix (ECM) protein fibronectin, hydrophobicity, and hemolysis. We present results from experiments where staphylococci were exposed to healthy female urine; however, in initial experiments, we confirmed that exposure to male or female urine affected MRSA-1369 adherence to human bladder epithelial cells and transcription of specific MRSA-1369 genes in a similar manner.

Overall, our study provides important insights into the effects of urinary microenvironment on MRSA physiology. However, we acknowledge important limitations that changes in mRNA transcripts do not guarantee corresponding changes in protein levels and that examination of MRSA virulence at early time points following *in vitro* exposure to HU provides a predictive snapshot into changes in MRSA physiology during initial phases of *in vivo* urinary tract colonization. The future research aimed at addressing these caveats will have to focus on examining transcriptomes and proteomes of both host and MRSA from bladder and kidney tissues at different time points after experimental induction of ascending UTI in a mouse model. In addition, identified correlations between human urine-mediated changes in virulence characteristics and the changes in gene expression must be confirmed in the future by comparing specific gene deletion mutants with the wild type (WT) in both *in vitro* and *in vivo* setups.

RESULTS

***S. aureus* strains grow in human urine.** We compared CFU in TSB control and in human urine (HU) at different time points up to 24 h to confirm that MRSA-1369, PUTS-1, and USA300 were not inhibited by human urine (Fig. 1). To minimize nutrient carryover from TSB to HU in our growth curve experiments, overnight cultures of *S.*

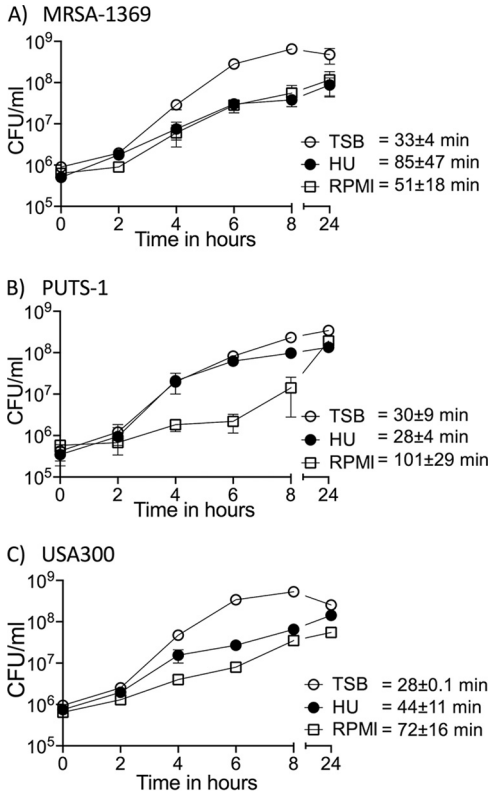

FIG 1 *S. aureus* strains are able to grow in human urine. (A) MRSA-1369, (B) PUTS-1, and (C) USA300 were cultivated in TSB, HU, or base RPMI. Bacterial growth was monitored by CFU enumeration over a period of 24 h. For each time point, average CFU/ml (two biological replicates) ± standard deviation (SD) is shown. Also shown is average doubling time ± SD for each strain in TSB, HU, or base RPMI.

aureus in TSB were washed with sterile phosphate-buffered saline (PBS) before inoculating $\leq 10^6$ CFU/ml in fresh TSB, HU, or RPMI. MRSA-1369 and USA300 cultivated in HU grew more slowly than did respective controls in nutrient-rich TSB, although this change was not significant statistically. In contrast, PUTS-1 doubling time (DT) was similar in TSB control (DT = 30 ± 9 min) and in HU (DT = 28 ± 4 min). Compared to that of PUTS-1 in HU (DT = 28 ± 4 min), the DT of MRSA-1369 in HU (85 ± 47 min) was 3-fold higher, while that of USA300 (DT = 44 ± 11 min) was 1.6-fold higher, although these differences were also not statistically significant. These results are similar to those reported by Walker et al. (9).

We also examined growth of all strains in base RPMI, which was used as control medium in bladder epithelial cell adherence assay. Compared to that in TSB control, doubling time for RPMI cultures was 1.5-fold ($P = 0.3$) higher in MRSA-1369, 3.4-fold higher ($P = 0.08$) for PUTS-1, and 2.5-fold higher ($P = 0.06$) for USA300. In separate experiments, staphylococci cultivated in human urine for 24 h and then subcultured 1:100 in fresh HU showed robust growth for 24 h post-subculture, further confirming that nutrient carryover between TSB and HU did not aid bacterial growth (data not shown).

Effects of human urine on the virulence characteristics of *S. aureus* strains. Staphylococci produce a large arsenal of virulence factors to facilitate their colonization, persistence, and dissemination within the host and for evasion of immune defenses. Hence, in the next set of experiments, we examined the effects of 2-h-long exposure to HU on staphylococcal virulence.

Bacterial adherence is the first crucial step in an infection, as it facilitates colonization and subsequent invasion across the mucosal barrier. We compared *S. aureus* strains in HU with the control for the ability to adhere to the 5637 human bladder epithelial cell line (Fig. 2) and to ECM proteins fibrinogen and fibronectin (Fig. 3). We observed that in comparison to preexposure to TSB (control), preexposure to HU for 2 h did not affect adherence of

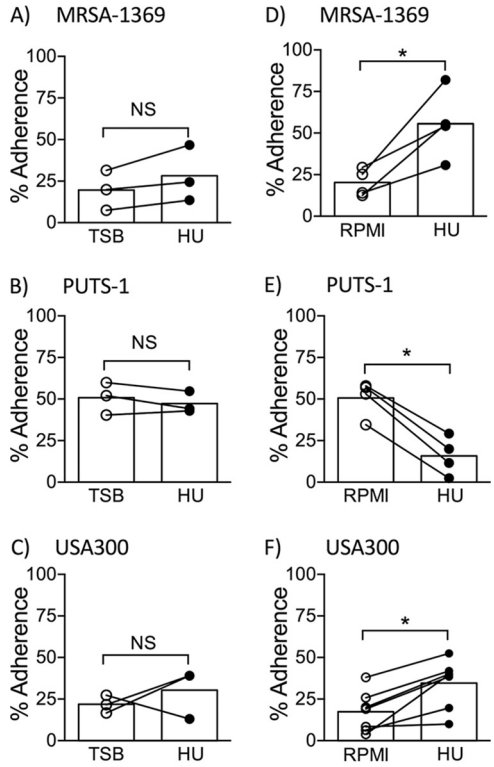

FIG 2 Human urine alters *S. aureus* adherence to human bladder epithelial cells in a strain-dependent manner. (A) MRSA-1369, (B) PUTS-1, and (C) USA300 preexposed to TSB or HU for 2 h were added to the monolayers of 5637 human bladder epithelial cell line. In separate experiments, (D) MRSA-1369, (E) PUTS-1, and (F) USA300 were added to 5637 monolayers overlaid with base RPMI (control) or HU. After 2-h-long incubation at 37°C, cell-adherent bacteria were enumerated. Percent adherence for biological replicates (each with two or more technical replicates) is reported as scatter diagram with mean shown as histogram. Statistical significance was determined by paired *t* test. For all figures, * refers to $P < 0.05$. NS, not significant.

MRSA1369, PUTS-1, or USA300 to bladder epithelial cells (Fig. 2A to C). We then tested *S. aureus* bladder epithelial adherence in a more life-like simulated bladder microenvironment setup wherein 5637 cells were overlaid with either human urine or base RPMI as described previously (11). Here, log-phase cultures of staphylococci were washed in sterile PBS before simulated bladder microenvironment was infected in the presence of either RPMI or HU. HU significantly increased adherence of MRSA strains MRSA-1369 and USA300 to bladder epithelial cells (Fig. 2D and F). In contrast, percent adherence for PUTS-1 in HU was significantly reduced compared to the percent adherence of the RPMI control (Fig. 2E). Of note, urine from healthy male volunteers also significantly induced adherence of MRSA-1369 to 5637 bladder epithelial cells (data not shown). When preexposed to HU for 2 h, all three strains showed modest but statistically insignificant reduction in fibrinogen binding (Fig. 3A to C). In contrast, HU preexposure significantly reduced fibronectin binding by MRSA1369, PUTS-1, and USA300 (Fig. 3D to F). The amount of fibrinogen/fibronectin was chosen based on our previous publication examining staphylococcal binding to fibronectin using same *in vitro* binding assay protocol (12); Walker et al. have also shown that a similarly low concentration of fibrinogen (18.5 μg/ml) induces staphylococcal agglutination (13).

Next, we used microbial adhesion to hydrocarbons test (MATH) (14) to analyze changes in staphylococcal surface hydrophobicity induced by HU. In this assay, TSB control and HU preexposed *S. aureus* strains were mixed with a hydrocarbon, hexadecane. At the end of 30 min incubation time, bacteria present in the aqueous phase were enumerated to estimate hydrophobicity. Significantly lower numbers of HU-exposed MRSA-1369 in comparison to those of the control were found in the aqueous

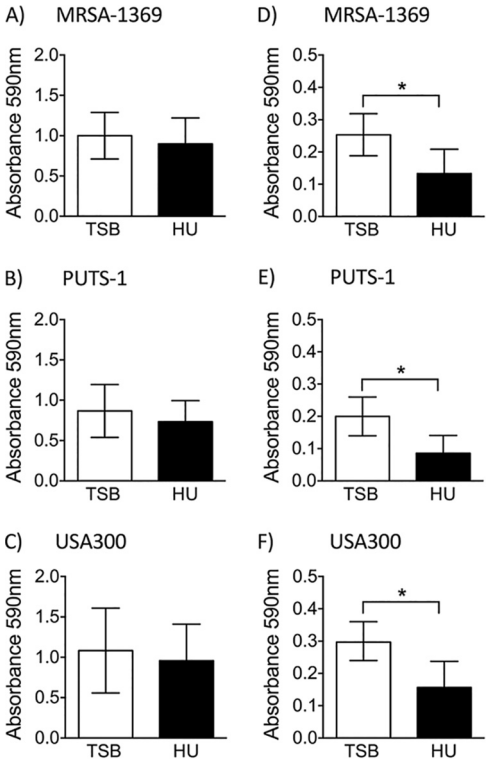

FIG 3 Human urine reduces staphylococcal adherence to ECM proteins. *S. aureus* strains preexposed to either TSB or HU for 2 h were incubated in plates coated with human fibrinogen (A to C) or human fibronectin (D to F). After vigorous washing, adherent bacteria were quantified by crystal violet staining and measurement of absorbance at 590 nm. Mean absorbance ± SD values were compared by paired *t* test.

phase, indicating that human urine increases hydrophobicity of MRSA-1369 (Fig. 4A). Reduction in surface hydrophobicity is an important immune evasion mechanism used by staphylococci to avoid killing by antimicrobial peptides (15); however, we did not observe corresponding changes in the killing of MRSA-1369 by human cathelicidin, LL37 (data not shown). Exposure to HU did not significantly alter surface hydrophobicity of either PUTS-1 (Fig. 4B) or USA300 (Fig. 4C).

S. aureus secretes numerous cytolytic toxins to target and kill mammalian cells by damaging their plasma membrane. The cytolytic activity contributes to pathogenesis by helping MRSA evade phagocyte-mediated killing (16). To visualize whether exposure to human urine alters staphylococcal cytolytic activity, we incubated 2-fold dilutions of *S. aureus* strains (starting from 10^8 CFU/ml) preexposed for 2 h to either HU or TSB control with sheep red blood cells (RBCs) at 37°C. After incubation, we quantified hemoglobin released in the supernatant spectrophotometrically. Both MRSA-1369 (Fig. 5A) and USA300 (Fig. 5C) preexposed to HU exhibited ~1.5-fold higher hemolysis compared to that of TSB controls. In a striking contrast, control PUTS-1 exhibited very low hemolysis activity, which was not altered by preexposure to HU (Fig. 5B).

Staphylococcal cell wall homeostasis involves two competing processes, namely, cell wall synthesis governed by cell wall synthesizing enzymes (also known as penicillin-binding proteins) and autolysis regulated by murein hydrolases (also known as autolysins). *S. aureus* autolysis is upregulated in response to adverse physiological conditions, including exposure to cell wall inhibitor β lactam antibiotics (17). We did not observe significant changes in autolysis in any of the staphylococcal strains following 2-h-long cultivation in HU (data not shown).

Effects of human urine on the gene expression in *S. aureus* strains. Using quantitative real-time PCR (qRT-PCR), we compared expression of select genes from MRSA-

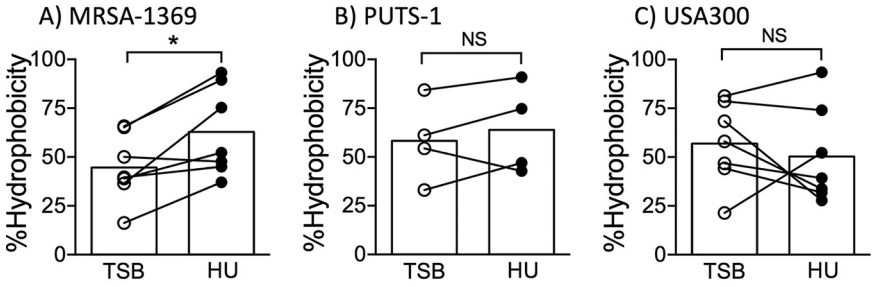

FIG 4 Effects of human urine on *S. aureus* hydrophobicity. Following preexposure to either TSB or human urine (HU), surface hydrophobicity was quantified for (A) MRSA-1369, (B) PUTS-1, and (C) USA300. Percent hydrophobicity (with average shown as histogram) is reported. Statistical significance was determined by paired *t* test.

1369, PUTS-1, and USA300 following exposure to human urine for 2 h (Fig. 6). The genes selected for this analysis include virulence genes *atl* (encoding autolysin), *clfAB* (encoding clumping factor A and B), *fib* (encoding fibrinogen-binding protein), *fnbA* (encoding fibronectin-binding protein A), and *hla* (encoding hemolysin) and transcriptional regulators *agrC* (encoding accessory gene regulator) and *sarA* (encoding staphylococcal accessory regulator). Genes that were 2-fold up- or downregulated (marked by dotted lines in Fig. 6) were considered significant. As shown in Fig. 6A, HU altered in a strain-specific manner the expression of *agrC*, *clfA*, *fib* (≥2-fold altered in PUTS-1, unchanged in others), and *hla* (≥3-fold upregulated in MRSA-1369 and USA300, 2.3-fold upregulated in PUTS-1). In contrast, the expression of *clfB* and *fnbA* was downregulated by human urine to a similar extent in all three *S. aureus* strains (Fig. 6A). Similar to qRT-PCR results from female urine, exposure of MRSA-1369 to HU from male volunteers significantly suppressed expression of *sarA*, *clfB*, and *fnbA* while significantly inducing *hla* expression (data not shown).

To delineate changes in gene expression during epithelial adherence experiment where we exposed staphylococci to HU or RPMI, we analyzed gene expression in staphylococci exposed for 2 h to HU relative to that in RPMI control (Fig. 6B). Relative to RPMI control, HU-exposed staphylococci showed ≥2-fold increased transcription of *sarA*, *clfA*, and *hla* (*hla* transcription unchanged in PUTS-1) and ≥2-fold decreased transcription of *atl* and *clfB* (Fig. 6B). In contrast, relative to that in RPMI control, *fib* was upregulated in HU-exposed USA300 and MRSA1369 and downregulated in HU-exposed PUTS-1 (Fig. 6B).

RNA-Seq and read mapping. We used RNA-Seq to quantify differential gene expression by assessing variation across the transcriptome for MRSA-1369 cultivated in human urine versus that in TSB control. MRSA-1369 was selected for RNA-Seq analysis because it is a clinical isolate from a patient suffering from CAUTI (9). RNA was isolated from three independent biological replicates in each treatment. Whole-transcriptome sequencing with rRNA depletion resulted in an average of 25.2 million 150-bp paired-end reads per sample (range: 21.6 to 31.0 million reads). After adapter trimming and quality filtering, we retained an average of 96.1% of reads (95.4 to 97%) per library.

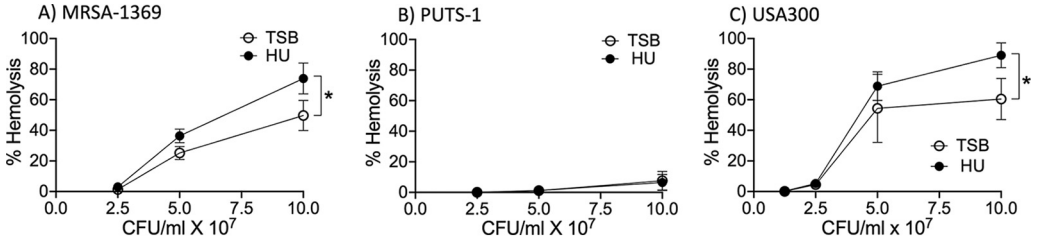

FIG 5 Human urine induces lysis of sheep RBCs by *S. aureus* in a strain-dependent manner. Mid-log cultures of (A) MRSA-1369, (B) PUTS-1, and (C) USA300 were cultivated for 2 h in either TS broth (TSB) or human urine (HU). Two-fold dilutions of bacteria (from 10^8 CFU/ml to 1.25×10^7 CFU/ml) were then incubated with sheep RBCs for 2 h at 37°C. Intact RBCs were centrifuged. The absorbance at 420 nm of supernatant was reported as percentage of total hemolysis (induced by Triton X-100 treatment). Average percent hemolysis (at least three biological replicates, each with at least two technical replicates) ± SD is reported. Statistical significance was determined by paired *t* test.

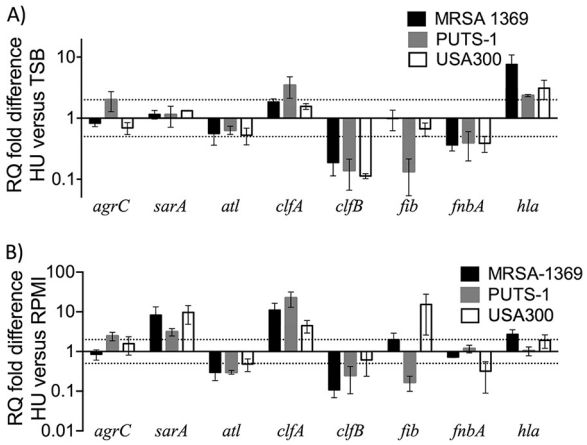

FIG 6 qRT-PCR results for *S. aureus* strains following cultivation in human urine. We used quantitative real-time PCR with normalization to 16S rRNA to determine mRNA transcript levels for specific virulence and associated genes (indicated on *x* axis) in MRSA-1369, PUTS-1, and USA300 following 2-h-long exposure to TSB or HU (A) or for MRSA-1369 exposed to RPMI and HU (B). RQ values were calculated by comparative threshold cycle ($\Delta\Delta C_T$) algorithm. RQ fold differences over transcript levels from TSB control (A) or RPMI control (B) are presented as the average of at least two biological replicates (each with three technical repeats) ± standard deviation. Dotted lines indicate 2-fold up- or down-regulation.

Subsequently, an average of 24.1 million reads (20.6 to 30 million reads) per library were successfully mapped to the methicillin-resistant *Staphylococcus aureus* USA300 reference genome (GenBank accession number CP000255.1), with an average of only 1.5% of reads (0.9 to 2.8%) mapping to ribosomal genes. We mapped to the USA300 genome because both MRSA-1369 and USA300 belong to sequence type 8 (ST8). The libraries had an average estimated depth of coverage of 9,166-fold (7,842× to 11,384×), with only 1.7% of genes having fewer than 10 mapped reads (2,585/2,631 genes with sufficient sample size for determining differential expression). For comparisons of TSB versus HU, Euclidean distances between samples (Fig. S1 in the supplemental material) and principal-component analysis (Fig. S2) revealed that expression patterns in biological replicates of each treatment group were more similar to each other than they were to those in biological replicates of the contrasting treatment group. Detailed RNA-Seq data including normalized counts for triplicate samples, $\log_2$(fold change), and adjusted *P* values (P_{adj}) are presented in Table S1. All instances of $\log_2$(fold change) are abbreviated as $\log_2$(FC) and presented as HU samples relative to the TSB control. Of these, 861 genes showed significant changes in gene expression (defined as $|\log_2 FC| > 1$ and $P_{adj} \leq 0.05$). These are categorized into 461 significantly upregulated genes (Table S2) and 400 significantly downregulated genes (Table S3). RNA-Seq results were confirmed by qRT-PCR-based analysis of expression of a panel of 15 overlapping genes. Fold change was correlated across these genes with r^2 equal to 0.68 (Fig. S3).

MRSA-1369 differential gene expression in human urine. Healthy human urine is made of a low concentration of amino acids and short peptides, trace amounts of transition metals, and more than 2,500 metabolites (18, 19). To examine the metabolic adaptations in MRSA-1369 in response to the nutrient-limiting growth conditions in HU, we compared the expression of metabolic genes in TSB control and human urine-exposed MRSA-1369. We observed that 2-h-long exposure to glucose-free HU results in the elimination of catabolite repression marked by significant upregulation of the gene encoding catabolite control protein (*ccpA*) and activation of genes encoding enzymes involved in the catabolism of amino acids alanine (*ald*), glutamate (*gudB*), arginine (*rocFD*), histidine (*hutHIUG*), proline (*putAP*), and serine (*sdaAA*,*AB*) (Table 1). We also observed that the tricarboxylic acid (TCA) cycle (Gene Ontology [GO]: 0006099) was one of the significantly enriched GO terms (Fig. 7A). More specifically, in comparison to TSB control, MRSA-1369 in HU exhibited significantly increased expression of

TABLE 1 RNA-Seq results for genes involved in amino acid catabolism

Gene ID	Gene symbol	$\log_2$(FC)[a]	GenBank annotation
SAUSA300_0008	*hutH*	2.44	Histidine ammonia-lyase
SAUSA300_0184	*argB*	−1.04	Acetylglutamate kinase
SAUSA300_0860	*rocD*	3.94	Ornithine aminotransferase
SAUSA300_0861	*gudB*	3.37	NAD-specific glutamate dehydrogenase
SAUSA300_1331	*ald*	−5.81	Alanine dehydrogenase
SAUSA300_1655	*ald*	3.19	Alanine dehydrogenase
SAUSA300_1682	*ccpA*	2.31	Catabolite control protein A
SAUSA300_1711	*putA*	3.94	Proline dehydrogenase
SAUSA300_1883	*putP*	1.25	High affinity proline permease
SAUSA300_2114	*rocF*	3.86	Arginase
SAUSA300_2277	*hutI*	4.74	Imidazolonepropionase
SAUSA300_2278	*hutU*	5.07	urocanate hydratase
SAUSA300_2281	*hutG*	1.36	Formimidoylglutamase
SAUSA300_2469	*sdaAA*	2.10	L-Serine dehydratase, iron-sulfur-dependent, alpha subunit
SAUSA300_2470	*sdaAB*	2.14	L-Serine dehydratase, iron-sulfur-dependent, beta subunit
SAUSA300_2571	*argR*	−2.03	Arginine repressor

[a]Only values where absolute $\log_2$(fold change) is greater than 1 and *P* is less than 0.05 are shown. Positive values indicate greater expression in the human urine treatment, and negative values indicate greater expression in the TSB control.

genes encoding enzymes in the tricarboxylic acid (TCA) cycle, such as succinate dehydrogenase (*sdhCAB*), succinyl-coA synthase (*sucCD*), 2-oxoglutarate dehydrogenase (*sucBA*), isocitrate dehydrogenase (*icd*), aconitate hydratase (*acnA*), citrate synthase (*gltA*), fumarate hydratase (*fumC*), and malate:quinone-oxidoreductase (*mqo*). Two-hour-long exposure to HU also increased transcription of genes encoding phosphoenolpyruvate carboxykinase (*pckA*), which catalyzes the first irreversible step in gluconeogenesis by converting oxaloacetate into phosphoenol pyruvate and pyruvate synthase (also known as pyruvate ferredoxin oxidoreductase), which catalyzes conversion of pyruvate into acetyl coenzyme A (acetyl-coA), the substrate for the TCA cycle (Table 2).

Given the status of MRSA as a major human pathogen, we were interested in analyzing RNA-Seq data to define the changes in virulence genes and associated regulators following 2-h-long cultivation in human urine. To achieve this objective, we focused on genes categorized into KEGG pathway defined as "*Staphylococcus aureus* infection" (saa05150) and on genes experimentally shown to play a role in MRSA infection (Table 3). In HU-exposed MRSA-1369, we observed significant downregulation of genes encoding surface proteins involved in colonization such as *sasG/E* and clumping factor B (*clfB*), cytolytic toxins Panton-Valentine leukocidin (*lukF/S*), *seq* superantigen, and *eta* protease. In contrast, HU significantly upregulated expression of genes encoding surface proteins clumping factor A (*clfA*), fibrinogen-binding protein (*efb*), and cytolytic α-hemolysin precursor (*hla*) and γ-hemolysin (*hlgA/B/C*). In addition, HU also significantly altered expression of transcriptional regulators such as *codY*, *agr* quorum sensing system (*agrDCA*), *sarA* family regulators (*rot*, *sarA*, *mgrA*), two-component systems *saeS/R* and *lytR/S*, stress-related gene *ctsR*, and heat shock protein-encoding genes *clpPCB*, *dnaJ/K*, *grpE*, and *groL/ES* (Table 3).

Human urine induced significantly higher expression of MRSA-1369 genes in pathways for acquisition and export of transition metals iron, nickel, and zinc, which are essential nutrients. The expression of genes encoding zinc transporters *znuB/C* and SAUSA300_2315, cobalt-nickel transporters *cntFDCB*, *opp1A*, and oligopeptide transporters *oppBCDFAA* was upregulated in MRSA-1369 exposed to HU for 2 h (Table 4). As shown in Table 5, HU also induced upregulation of *sbnABCDEFGHI* and *sirA/B* involved in the production and import of siderophore staphyloferrin B, respectively, *fhuC/B* involved in siderophore transport, *isdCDEF*, *srtB* from iron surface determinant *isd* heme acquisition system, *sstABCD* from catechol/catecholamine iron transporter

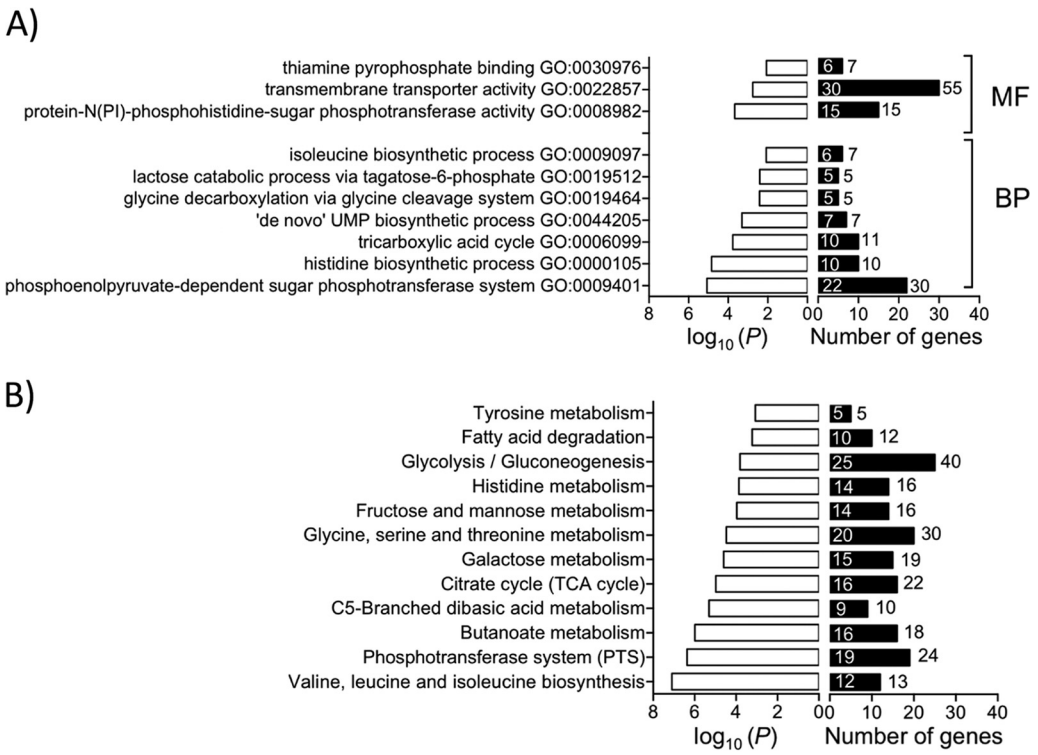

FIG 7 Enrichment analysis of RNA-Seq data. (A) Gene ontology (GO) terms significantly enriched for differentially expressed genes (DEG) at a *P* value of <0.01 are shown. For each GO category, the number of DEG (differentially expressed genes) is shown inside the histogram, while the number of total genes in each category is shown next to each histogram. MF, molecular function; BP, biological process. (B) KEGG pathways significantly enriched for DEG at a *P* value of <0.01 are shown. For each KEGG pathway, the number of DEG is shown inside the histogram while the total number of annotated genes is shown next to the histogram.

system, and *htsCBA* importer of staphyloferrin A (20, 21). Beyond our targeted hypotheses above, RNA-seq analysis of HU-exposed replicates also revealed significant enrichment of 10 GO categories (Fig. 7A) and 12 KEGG pathways (Fig. 7B).

DISCUSSION

An overarching objective of our research is to delineate the effects of the growth-limiting, hostile microenvironment of the urinary tract on the physiology of various bacterial pathogens. Here, we examined virulence characteristics and gene expression of various *S. aureus* strains using healthy female urine as a culture medium to mimic conditions encountered during the colonization of human urinary tract. The specific strains analyzed in this study include two urinary isolates, MRSA-1369 and PUTS-1, and a prototypical MRSA strain, USA300, all of which were able to grow in HU as previously reported (9), although based on the comparison of doubling times for each strain, PUTS-1 growth in HU is faster than the growth of either MRSA-1369 or USA300 in HU. Given that PUTS-1 is a clinical isolate from a woman with asymptomatic bacteriuria, our results match previous reports that asymptomatic bacteriuria strains of uropathogenic *Escherichia coli* and *Streptococcus agalactiae* exhibit rapid growth in human urine compared to that of those causing cystitis (22, 23). Our observations further suggest that the induction of specific virulence characteristics by human urine is strain dependent. In addition, we also compared the global transcriptome profiles of uropathogenic strain MRSA-1369 exposed *in vitro* to either human urine or nutrient-rich culture medium TSB (control). The RNA-Seq observations constitute the first step in defining molecular basis for results from virulence assays as discussed below.

S. aureus strains infecting humans secrete numerous cytolytic exotoxins, such as α-hemolysin and leukotoxins, as well as cytolytic peptides called phenol soluble

TABLE 2 RNA-Seq results for genes encoding enzymes catalyzing glycolysis, gluconeogenesis, and TCA cycle

Gene ID	Gene symbol	$\log_2$(FC)[a]	GenBank annotation	KEGG pathway categorization[b]		
				Gly	Neo	TCA
SAUSA300_0757	*pgk*	−2.10	Phosphoglycerate kinase	X	X	
SAUSA300_0759	*gpmI*	−2.03	2,3-bisphosphoglycerate-independent phosphoglycerate mutase	X	X	
SAUSA300_0756	*gap*	−1.97	Glyceraldehyde-3-phosphate dehydrogenase, type I	X	X	
SAUSA300_0758	*tpiA*	−1.95	Triosephosphate isomerase	X	X	
SAUSA300_2079	*fba*	−1.21	Fructose bisphosphate aldolase	X	X	
SAUSA300_1644	*pyk*	−1.01	Pyruvate kinase	X		
SAUSA300_1633	*gap*	4.42	Glyceraldehyde-3-phosphate dehydrogenase, type I	X	X	
SAUSA300_1246	*acnA*	1.33	Aconitate hydratase			X
SAUSA300_1183		1.52	Pyruvate ferredoxin oxidoreductase, beta subunit			X
SAUSA300_1182		1.69	Pyruvate ferredoxin oxidoreductase, alpha subunit			X
SAUSA300_2312	*mqo*	1.78	Malate:quinone-oxidoreductase			X
SAUSA300_1046	*sdhC*	1.97	Succinate dehydrogenase, cytochrome b-558 subunit			X
SAUSA300_1047	*sdhA*	2.16	Succinate dehydrogenase, flavoprotein subunit			X
SAUSA300_1048	*sdhB*	2.29	Succinate dehydrogenase, iron-sulfur protein			X
SAUSA300_1801	*fumC*	2.69	Fumarate hydratase, class II			X
SAUSA300_2455		2.86	Putative fructose-1,6-bisphosphatase		X	
SAUSA300_1641	*gltA*	3.43	Citrate synthase II			X
SAUSA300_1640	*lcd*	3.48	Isocitrate dehydrogenase, NADP-dependent			X
SAUSA300_1306	*sucA*	3.53	2-Oxoglutarate dehydrogenase, E1 component			X
SAUSA300_1305	*sucB*	3.62	2-Oxoglutarate dehydrogenase, E2 component, dihydrolipoamide succinyltransferase			X
SAUSA300_1139	*sucD*	4.09	Succinyl-coA synthetase, alpha subunit			X
SAUSA300_1731	*pckA*	4.19	Phosphoenolpyruvate carboxykinase (ATP)		X	
SAUSA300_1138	*sucC*	4.35	Succinyl-coA synthetase, beta subunit			X

[a]Values where absolute $\log_2$(fold change) is greater than 1 and *P* is less than 0.05 are shown.
[b]An "X" indicates that a gene belongs to a specific KEGG pathway: saa00010, glycolysis (Gly) and gluconeogenesis (Neo); saa00020, tricarboxylic cycle (TCA).

modulins, which play an important role in staphylococcal pathogenesis by facilitating tissue damage, immune evasion, and dissemination (16). We observed upregulation of *hla* encoding α-hemolysin and *hlgACB* cluster encoding γ-hemolysin, both of which are known to target a broad range of host cells, including red blood cells (24, 25). The *hla* gene is expressed by most clinical isolates of MRSA, and its expression level is correlated with the disease severity (26). Moreover, α-hemolysin is known to be essential for MRSA virulence in animal models of skin and soft tissue infections (SSTI), pneumonia, and bacteremia (24). The γ-hemolysin belongs to the leukotoxin family of cytolysins, which are made of two different protein components that assemble to form β barrel pores in the host plasma membrane. The γ-hemolysin is highly prevalent in *S. aureus* clinical isolates from human nose and blood (25). While *hlgACB* genes are upregulated in human blood, the contribution of γ-hemolysin to staphylococcal virulence is modest, as shown by the results from infection experiments comparing WT MRSA with Δ*hlgACB* mutant defective in γ-hemolysin production in animal models of eye infection (27), bacteremia (28), and septic arthritis (29). The increased expression of *hla* and *hlgACB* in HU and corresponding increase in hemolytic activity suggest that either one or both toxins may play an important role in the urinary pathogenesis of MRSA-1369. It will be worthwhile for the future research to compare uropathogenesis of MRSA-1369 WT and *hla* knockout (KO) strains in a mouse model. Equally interesting will be experiments examining whether the absence of hemolytic activity in PUTS-1 can be explained by

TABLE 3 RNA-Seq results for virulence genes categorized into KEGG pathway saa05150 "*Staphylococcus aureus* infection" and important transcriptional regulators

Gene ID	Gene symbol	$\log_2$(FC)[a]	GenBank annotation
MSCRMM colonization			
SAUSA300_2435	*sasG_E*	−1.25	Cell wall surface anchor family protein
SAUSA300_2436	*sasG_E*	−1.51	Putative cell wall surface anchor family protein
SAUSA300_2565	*clfB*	−1.08	Clumping factor B
Surface protein-encoding			
SAUSA300_0772	*clfA*	1.27	Clumping factor A
SAUSA300_1055	*efb*	3.09	Fibrinogen-binding protein
SAUSA300_1920	*chs*	−1.33	Chemotaxis-inhibiting protein CHIPS
SAUSA300_1101		1.24	Putative fibronectin/fibrinogen-binding protein
SAUSA300_1052	*efbC*	3.19	Fibrinogen-binding protein
Antimicrobial activity			
SAUSA300_0647	*vraF*	−1.07	CAMP transport system ATP-binding protein
SAUSA300_0835	*dltA*	−1.40	D-Alanine-activating enzyme/D-alanine-D-alanyl
Cytolytic toxins			
SAUSA300_2365	*hlgA*	6.80	γ-Hemolysin component A
SAUSA300_2366	*hlgC*	3.63	γ-Hemolysin component C
SAUSA300_2367	*hlgB*	3.14	γ-Hemolysin component B
SAUSA300_1058	*hla*	3.52	α-Hemolysin precursor
Superantigens/superantigen-like protein-encoding			
SAUSA300_0801	*seq*	−1.04	Staphylococcal enterotoxin Q
SAUSA300_1065	*eta*	−1.52	Exfoliative toxin A
Transcriptional regulator-encoding and two-component system-encoding			
SAUSA300_0254	*lytS*	−1.59	Sensor histidine kinase
SAUSA300_0255	*lytR*	−2.29	Sensory transduction protein
SAUSA300_0507	*ctsR*	3.15	Transcriptional regulator
SAUSA300_0605	*sarA*	1.51	Staphylococcal accessory regulator A
SAUSA300_0672	*mgrA*	−1.95	Transcriptional regulator, MarR family
SAUSA300_0690	*saeS*	2.13	Sensor histidine kinase
SAUSA300_0691	*saeR*	2.49	DNA-binding response regulator
SAUSA300_1148	*codY*	1.45	GTP-sensing transcriptional pleiotropic repressor
SAUSA300_1514	*fur*	1.26	Ferric uptake regulation protein
SAUSA300_1542	*hrcA*	3.58	Heat-inducible transcription repressor
SAUSA300_1708	*rot*	1.98	Staphylococcal accessory regulator
SAUSA300_1990	*agrD*	1.09	Accessory gene regulator protein D
SAUSA300_1991	*agrC*	1.02	Accessory gene regulator protein C
SAUSA300_1992	*agrA*	1.05	Accessory gene regulator protein A

[a]Only values where absolute $\log_2$(fold change) is greater than 1 and *P* is less than 0.05 are shown. Positive values indicate greater expression in the human urine treatment, and negative values indicate greater expression in the TSB control.

the inactivation of one or more cytolytic toxin genes and whether comparatively rapid growth of PUTS-1 in HU compensates for the lack of hemolysis offering it a competitive advantage in asymptomatic colonization of the urinary tract.

Multiple nonspecific and specific mechanisms of adherence facilitate early steps of staphylococcal colonization of host tissue by promoting bacterial attachment to host cells and extracellular matrix proteins. Nonspecific mechanisms include changes in surface charge and hydrophobicity, while specific mechanisms include number of cell wall anchored adhesins (MSCRAMMs; microbial surface components recognizing adhesive matrix molecules), which specifically adhere to ECM proteins collagen, fibrinogen, and fibronectin (30). Adherence to bladder epithelium is the first important step in urinary pathogenesis, as it prevents removal of uropathogens by the gush of urine. HU specifically induced adherence to human bladder epithelial cells by MRSA-1369 and USA300. The hydrophobicity was significantly higher in MRSA-1369 cultivated in human urine. Based on gene expression data, the increased adherence in MRSA strains cultivated in HU could potentially be mediated by the product of one or more of the surface adhesin genes *clfA*, *efb*, *efbC*, and SAUSA300_1101. In contrast, binding to

TABLE 4 RNA-Seq results for genes categorized into KEGG pathway saa02010 "ABC transporters"

Gene ID	Gene symbol	log_2(FC)[a]	GenBank annotation
Mineral and organic iron transport			
SAUSA300_0219		−1.345	Putative iron compound A C transporter, iron compound-binding protein
SAUSA300_0999	*potA*	2.17	Spermidine/putrescine ABC transporter, ATP-binding protein
SAUSA300_1000	*potB*	2.48	Spermidine/putrescine ABC transporter, permease protein
SAUSA300_1001	*potC*	1.92	Spermidine/putrescine ABC transporter, permease protein
SAUSA300_1002	*potD*	1.05	Spermidine/putrescine ABC transporter, spermidine/putrescine-binding protein
Oligosaccharide, polyol, and lipid transport			
SAUSA300_0209		1.78	Putative maltose ABC transporter, maltose-binding protein
SAUSA300_0210		1.89	Maltose ABC transporter, permease protein
SAUSA300_0211		1.73	Maltose ABC transporter, permease protein
SAUSA300_0263	*rbsD*	1.99	Ribose permease
Phosphate and amino acid transport			
SAUSA300_1280	*pstB*	1.21	Phosphate ABC transporter, ATP-binding protein
Cysteine transport			
SAUSA300_2357		−1.24	ABC transporter, ATP-binding protein
SAUSA300_2358		−1.11	ABC transporter, permease protein
SAUSA300_2359		−1.19	Amino acid ABC transporter, amino acid-binding protein
Oligopeptide transport			
SAUSA300_0887	*oppB*	1.11	Oligopeptide ABC transporter, permease protein
SAUSA300_0888	*oppC*	1.25	Oligopeptide ABC transporter, permease protein
SAUSA300_0889	*oppD*	1.36	Oligopeptide ABC transporter, ATP-binding protein
SAUSA300_0890	*oppF*	1.42	Oligopeptide ABC transporter, ATP-binding protein
SAUSA300_0891	*oppA*	1.41	Oligopeptide ABC transporter, substrate-binding protein
SAUSA300_0892	*oppA*	1.20	Oligopeptide ABC transporter, oligopeptide-binding protein
Nickel transport			
SAUSA300_2407	*cntF/nikE*	1.70	Oligopeptide ABC transporter, ATP-binding protein
SAUSA300_2408	*cntD/nikD*	1.90	Oligopeptide ABC transporter, ATP-binding protein
SAUSA300_2409	*cntC/nikC*	1.89	Oligopeptide ABC transporter, permease protein
SAUSA300_2410	*cntB/nikB*	2.80	Oligopeptide ABC transporter, permease protein
SAUSA300_2411	*opp-1A/nikA*	2.99	Oligopeptide permease, peptide-binding protein
Iron siderophore transport			
SAUSA300_2134		1.49	Iron compound ABC transporter, permease protein
SAUSA300_2135		1.70	Iron compound ABC transporter, permease protein
SAUSA300_2136		2.86	Iron compound ABC transporter, iron compound-binding protein
Zinc transport			
SAUSA300_1515		1.47	ABC transporter, permease protein
SAUSA300_1516		1.76	ABC transporter, ATP-binding protein
SAUSA300_2351		1.94	Zn-binding lipoprotein adca-like protein
Biotin transport			
SAUSA300_0977		−2.49	Cobalt transport family protein
Unclassified			
SAUSA300_1760	*epiG*	2.18	Lantibiotic epidermin immunity protein F
SAUSA300_1761	*epiE*	1.76	Lantibiotic epidermin immunity protein F
SAUSA300_1762	*epiF*	1.39	Lantibiotic epidermin immunity protein F
SAUSA300_2465		−1.41	ABC transporter, ATP-binding protein
SAUSA300_0647		−1.07	ABC transporter, ATP-binding protein
SAUSA300_0672		−1.95	Transcriptional regulator, MarR family

[a]Only values where absolute log_2(fold change) is greater than 1 and *P* is less than 0.05 are shown. Positive values indicate greater expression in the human urine treatment, and negative values indicate greater expression in the TSB control.

fibronectin was reduced in all three staphylococcal strains. This matches with gene expression results (qRT-PCR and RNA-Seq) showing that the expression of genes encoding principal fibronectin adhesins, fibronectin-binding protein (*fnbAB*), was downregulated in HU (relative to that in TSB) in MRSA-1369, PUTS-1, and USA300.

Clumping factor A and B (ClfA, ClfB) are important mediators of MRSA binding to fibrinogen (31). MRSA adherence to fibrinogen is implicated in the pathogenesis of

TABLE 5 RNA-Seq results for genes involved in iron transport

Gene ID	Gene symbol	$\log_2$(FC)[a]	GenBank annotation
SAUSA300_0633	*fhuA*	1.83	Ferrichrome transport ATP-binding protein FhuA
SAUSA300_0634	*fhuB*	1.08	Ferrichrome transport permease protein FhuB
SAUSA300_0116	*sirB*	1.84	Iron compound ABC transporter, permease protein SirB
SAUSA300_0117	*sirA*	2.30	Iron compound ABC transporter, iron compound-binding protein SirA
SAUSA300_0118	*sbnA*	2.64	Pyridoxal-phosphate dependent enzyme superfamily
SAUSA300_0119	*sbnB*	2.29	Ornithine cyclodeaminase
SAUSA300_0120	*sbnC*	2.16	Siderophore biosynthesis protein, IucC family
SAUSA300_0121	*sbnD*	1.90	Putative drug transporter
SAUSA300_0122	*sbnE*	1.54	Siderophore biosynthesis protein, IucA/IucC family
SAUSA300_0123	*sbnF*	1.37	Siderophore biosynthesis protein, IucC family
SAUSA300_0124	*sbnG*	1.42	HPCH/HPAI aldolase family protein
SAUSA300_0125	*Sbnh*	1.27	Pyridoxal-dependent decarboxylase
SAUSA300_0126	*sbnI*	1.03	Conserved hypothetical protein
SAUSA300_0718	*sstA*	2.45	Iron compound ABC transporter, permease
SAUSA300_0719	*sstB*	2.52	Iron compound ABC transporter, permease protein
SAUSA300_0720	*sstC*	2.88	Putative iron compound ABC transporter, ATP-binding protein
SAUSA300_0721	*sstD*	3.77	Transferrin receptor
SAUSA300_1030	*isdC*	2.59	Iron transport associated domain protein
SAUSA300_1031	*isdD*	2.01	Conserved hypothetical protein
SAUSA300_1032	*isdE*	2.31	Putative iron compound ABC transporter, iron compound-binding protein
SAUSA300_1033	*isdF*	1.39	Iron/heme permease
SAUSA300_1034	*srtB*	1.64	Sortase B
SAUSA300_1035	*isdG*	1.11	Conserved hypothetical protein
SAUSA300_2134	*htsC*	1.49	Iron compound ABC transporter, permease protein
SAUSA300_2135	*htsB*	1.70	Iron compound ABC transporter, permease protein
SAUSA300_2136	*htsA*	2.86	Iron compound ABC transporter, iron compound-binding protein

[a]Only values where absolute $\log_2$(fold change) is greater than 1 and *P* is less than 0.05 are shown. Positive values indicate greater expression in the human urine treatment, and negative values indicate greater expression in the TSB control.

CAUTI, as MRSA infection is shown to increase fibrinogen deposition on catheters and because Δ*clfB* deletion mutant in MRSA-1369 shows reduced bacterial burden on catheter implant in a mouse model of CAUTI (9). Interestingly, deletion of *clfA* (Δ*clfA*) does not affect bacterial burden on catheter implant compared to that of WT MRSA-1369 (9). Previous publications have used 100 μg/ml fibrinogen to assess binding by Gram-positive *S. aureus* and enterococci (9, 32); exposure of *S. aureus* clinical isolates to human plasma containing 400 μg/ml fibrinogen was also shown to significantly augment expression of MSCRAMM genes (33). However, 2-h-long, *in vitro* exposure to HU supplemented with either 20 or 100 μg/ml human fibrinogen did not significantly affect MRSA-1369 gene expression relative to HU alone (data not shown). This apparent discrepancy can be attributed to the presence of other host proteins in addition to fibrinogen in plasma. It is also worth noting that 2 h may not be a long enough exposure time for HU supplemented with 20 or 100 μg/ml fibrinogen to induce discernible changes in staphylococcal gene expression. In the light of this information, how our observations that HU (relative to both TSB and RPMI) mediates upregulation of *clfA* and downregulation of *clfB* expression may shape MRSA uropathogenesis warrants further evaluation at various early and late time points in a mouse model.

Urine is a nutrient-poor culture medium that is primarily made of urea, inorganic salts, creatinine, organic acids, small quantities of amino acids, trace amounts of transition metals, and other water-soluble waste products from blood. To colonize glucose-free urinary tract, *S. aureus* must switch to catabolism of amino acids via tricarboxylic acid (TCA) cycle to provide substrates for gluconeogenesis. In our experiments, staphylococci were cultured in standard TSB containing 14 mM glucose to obtain an inoculum high enough for discernible changes in virulence following various experimental exposures. Subculture of staphylococci from TSB to glucose-free HU marks a drop in glucose availability that is steeper than the drop in glucose observed in real-life as *S. aureus* switches from being a commensal in the nasopharynx (with reported average glucose level of 400 μM [34]) to a pathogen infecting glucose-free urinary tract. Nevertheless, the elimination of catabolite

TABLE 6 Strains used in this study

Strain	Isolation site	Resistance	Reference cited
MRSA 1369	Urine	Methicillin	9
PUTS-1 4-147	Urine, asymptomatic	Penicillin	9
USA300	Skin and soft tissue	Methicillin	36

repression resulting in the increased production of enzymes catalyzing amino acid catabolism, TCA cycle, and gluconeogenesis and oligopeptide transporters (*oppBCDFAA*) when MRSA-1369 was cultivated in HU implicates these central metabolic pathways in MRSA uropathogenesis. This is similar to previous reports showing that UPEC mutants ablated in oligopeptide and dipeptide transport as well as mutants lacking enzymes catalyzing TCA cycle or gluconeogenesis exhibit fitness defects in the mouse model of ascending UTI (35).

In addition, our results also implicate transporter systems for nickel, iron, and zinc in MRSA uropathogenesis. Both bacterial pathogens and their eukaryotic hosts require transition metals for survival; hosts exert a tight control over metal homeostasis as a defense mechanism against infections, while bacteria produce acquisition (iron siderophores) and export systems to chelate metals from the host. HU contains trace quantities of iron (0.089 μM/mM creatinine), nickel (0.0080 μM/mM creatinine), cobalt (0.0014 μM/mM creatinine), and zinc (0.46 μM/mM creatinine) (19). Thus, rapid upregulation of nickel, iron, and zinc transporter systems following 2-h-long exposure to HU, as shown by RNA-Seq analysis, may afford survival advantage to MRSA in the urinary tract

Most research has been focused on revealing the interactions between host immunity and MRSA virulence in the context of predominant MRSA infections of skin, soft tissue, and lungs. In contrast, MRSA-host interactions within the urinary environment are largely unexplored. To survive in the urinary niches, MRSA must rapidly adapt to unique challenges in the form of nutrient unavailability, mobilization of immune defenses, acidic pH, osmolarity, and shear stress due to urine flow. In this report, we have correlated alterations in virulence characteristics visualized by *in vitro* assays with changes in the expression of specific genes, which we acknowledge is only the first step in understanding MRSA physiology in the urinary tract. In the future, such correlations should be confirmed by comparing deletion mutants targeting specific genes with WT MRSA by *in vitro* virulence assays and in a mouse model of ascending UTI. Also warranted are studies examining the physiology of host as well as pathogen in the context of MRSA-infected urinary tract.

MATERIALS AND METHODS

Bacterial strains and culture conditions. *Staphylococcus aureus* strains used in this study are MRSA-1369, PUTS-1, and USA300 (Table 6) (9, 36). MRSA-1369 and PUTS-1 were generously gifted by Scott J. Hultgren and Jennifer N. Walker (Washington University School of Medicine in St. Louis). On the day of experiment, overnight cultures in tryptic soy broth (TSB with standard, 14 mM glucose) at 37°C and shaking at 200 rpm were diluted 1:10 and grown to optical density at 600 nm (OD_{600}) of 0.6. These are referred to as mid-log cultures.

Urine from healthy male and female volunteers (protocol approved by UL Lafayette IRB) was collected after informed consent was obtained from each volunteer. Urine was immediately filter-sterilized using a 0.22-μm filter and stored in 1.5-ml aliquots at –80°C. At the time of experiments, urine aliquots from three to five different donors were warmed to 37°C and mixed. Mid-log cultures were exposed to TSB (control), HU, base RPMI, or HU supplemented with 20 μg/ml or 100 μg/ml fibrinogen for 2 h at 37°C. HU refers to female urine.

After exposure, bacteria were centrifuged, washed in Dulbecco's phosphate-buffered saline (D-PBS), and used in various *in vitro* virulence assays and for RNA extractions as specified below. To enumerate the CFU/ml, we plated serial, 10-fold dilutions of bacteria on tryptic soy agar or CHROMagar.

Growth curve. *S. aureus* strains were inoculated at $<10^6$ CFU/ml in TSB, HU, or base RPMI at 37°C without shaking. CFU were enumerated by dilution plating at 0, 2, 4, 6, 8, and 24 h time points. For calculating doubling time (DT), CFU/ml values from 2 h and 4 h were used in the formula

$$\mathrm{DT} = \frac{\mathrm{Duration}\,(\log_2)}{\log\left(\frac{\mathrm{CFU}}{\mathrm{ml}}\,\mathrm{at}\ 4\,\mathrm{h}\right) - \log\left(\frac{\mathrm{CFU}}{\mathrm{ml}}\,\mathrm{at}\ 2\,\mathrm{h}\right)}$$

***In vitro* adherence assay.** The confluent monolayers of 5637 human bladder epithelial cell line (ATCC HTB-9) in 6-well cell culture plates were weaned (grown in base medium without fetal bovine

serum [FBS]) overnight before infection in two different experimental setups. In setup 1, staphylococci were exposed to TSB or HU for 2 h, washed, and then resuspended in base RPMI before infecting 5637 monolayers. In setup 2, monolayers overlaid with base RPMI (control) or HU were infected with mid-log-phase staphylococcal strains in TSB. We had previously described setup 2 as simulated bladder microenvironment (11). In both setups, MOI (multiplicity of infection) was set to 10. Plates were centrifuged to facilitate contact between MRSA and bladder cells. After incubation at 37°C for 2 h and 5% CO_2, supernatant was collected to determine nonadherent CFU by dilution plating. Monolayers were then washed 3 times with sterile PBS (containing Ca^{++}/Mg^{++}) to remove nonadherent bacteria. Adherent bacteria collected in sterile PBS containing 0.1% Triton X-100 were enumerated by dilution plating (37). Percent adherence was calculated as [adherent CFU/(adherent CFU + supernatant CFU)] × 100.

Fibrinogen- and fibronectin-binding assay. Assays to determine binding of MRSA to human ECM proteins fibrinogen or fibronectin were performed as described previously (12). In brief, a 96-well microtiter plate was coated overnight with 2-fold dilutions (20, 10, 5, 2.5, and 1.25 μg/ml) of 100 μl of human fibrinogen or fibronectin at 4°C. The wells were washed three times with 0.05% Tween 20 in sterile PBS and then blocked with 100 μl of 1% bovine serum albumin solution for 1 h at 37°C. The wells were washed again and 100 μl of MRSA (preexposed to HU or TSB control, adjusted to OD_{600} of 0.45) was added to at least duplicate wells. After incubation for 2 h at 37°C, nonadherent bacteria were removed by washing. The adherent bacteria were fixed with 100 μl of 25% formaldehyde for 30 min and stained with 100 μl of 1% crystal violet for 15 min at room temperature. After being washed with water and dried (37°C, 2 h) crystal violet was extracted with 70%-10% ethanol-methanol mixture. The absorbance was measured at 590 nm. Results for 20 μg/ml fibrinogen or fibronectin are shown.

Hydrophobicity test. Hydrophobicity was determined using MATH (microbial adhesion to hydrocarbon) assay, wherein *S. aureus* strains preexposed for 2 h to HU or TSB were centrifuged, resuspended in sterile D-PBS, and adjusted to OD_{600} of 0.6. One ml of each bacterial suspension was mixed with 125 μl hexadecane by vortexing for 1 min and incubated at room temperature for 30 min (38). The CFU/ml before addition of hexadecane (C_i) and CFU/ml in the aqueous phase (C_{aq}) after incubation with hexadecane were enumerated by dilution plating.

$$\%\,\text{hydrophobicity} = \left[(C_i - C_{aq})/C_i\right] \times 100$$

Antimicrobial peptide resistance assay. To determine the sensitivity of bacteria to human antimicrobial peptide (AMP) cathelicidin LL-37, *S. aureus* strains preexposed for 2 h to TSB or HU were washed and resuspended in sterile D-PBS supplemented with 20% TSB either without or with 50 μM LL-37 for 1 h. Bacteria were enumerated by dilution plating.

$$\%\,\text{AMP resistance} = \left(\text{CFU}_{\text{treated}}/\text{CFU}_{\text{untreated}}\right) \times 100$$

Hemolysis assay. Staphylococcal strains preexposed to TSB (control) or HU were used to generate 2-fold serial dilutions starting from 10^8 CFU/ml. Dilutions were mixed with equal volume of 1% sheep erythrocytes in PBS in 96-well conical bottom plate and incubated at 37°C. After 2 h, unlysed RBCs were pelleted at 3,000 rpm for 10 min and 100 μl supernatant was transferred to a fresh plate. Absorbance at 420 nm (A_{420}) was measured to estimate hemoglobin release (11). A_{420} readings for RBCs treated with PBS or 0.1% Triton X-100 were used to define baseline (A_{NC}) and 100% hemolysis (A_{PC}), respectively.

$$\%\,\text{hemolysis} = \left[(A_{\text{treatment}} - A_{NC})/(A_{PC} - A_{NC})\right] \times 100$$

Autolysis assay. Staphylococci preexposed to TSB or HU were resuspended in 0.2% Triton X-100 in sterile PBS and incubated at 37°C without shaking (39). We measured initial OD_{600} (OD_i) at the beginning of the experiment and then at 1-h intervals for 4 h (OD_t).

$$\%\,\text{autolysis} = \left[(OD_i - OD_t)/OD_i\right] \times 100$$

RNA extraction and quantitative real-time PCR (qRT-PCR). *S. aureus* strains in the mid-log phase of growth were exposed in TSB, HU, base RPMI, or HU supplemented with 20 or 100 μg/ml fibrinogen for 2 h at 37°C. Bacterial RNA was extracted using Ambion Ribopure kit (Thermofisher) and quantified using Synergy HTX multi-mode microplate reader (Biotek). Next, 1 μg RNA was reverse transcribed using the high-capacity cDNA reverse transcription kit (Applied Biosystems). qRT-PCR was carried out using SYBR green master mix (Applied Biosystems) in a StepOne Plus thermal cycler (Applied Biosystems). We used 16S rRNA as housekeeping gene. Relative quantification (RQ) values were calculated by comparing $\Delta\Delta C_T$ values of HU-exposed staphylococci with those of TSB control. The primers used for qRT-PCR are listed in Table 7.

Statistical analysis. Data from multiple replicates for each experiment are pooled together. Graphing and statistical analyses were done using GraphPad Prism 9 software. Results are expressed as the means ± standard deviation from data collected from two or more biological replicates each with two or more technical replicates. The data were compared using Student's *t* test as indicated. The difference between groups is considered significant if *P* is less than or equal to 0.05.

RNA-Seq data analysis. RNA for RNA-Seq was extracted as above. All library construction and initial analysis of differential expression were done by GENEWIZ (NJ, USA). Library construction included DNase treatment (TURBO DNase, ThermoFisher Scientific) and rDNA depletion (QIAseq FastSelect, Qiagen) followed by RNA fragmentation and random priming. cDNA synthesis (NEBNext Ultra II, New England

TABLE 7 Sequences of primers used for qRT-PCR in this study

Primer	Sequence
*16S*_F	GCG CTG CAT TAG CTA GTT GGT
*16S*_R	TGG CCG ATC ACC CTC TCA
*agrC*_F	CCA GCT ATA ATT AGT GGT ATT AAG TAC AGT AAA CT
*agrC*_R	AGG ACG CGC TAT CAA ACA TTT T
*ahpC*_F	GCA TGA CCA TTC AGA TGC AA
*ahpC*_R	CCA ATT CCG TCA GCG TTA AT
*atl*_F	TTT GGT TTC CAG AGC CAG AC
*atl*_R	TTG GGT TAA AGA AGG CGA TG
*clfA*_F	TTT CAA CAA CGC AAG ATA
*clfA*_R	GCT ACT GCC GCT AAA CTA
*clfB*_F	TTT GGG ATA GGC AAT CAT CA
*clfB*_R	TCA TTT GTT GAA GCT GGC TC
*fib*_F	GCG AAG GAT ACG GTC CAA GAG A
*fib*_R	CAA TTC GCT CTT GTA AGA CCA TT
*fnbA*_F	CCA GGT GGT GGT CAG GTT AC
*fnbA*_R	TGT GCT TGA CCA TGC TCT TC
*hla*_F	AGA AAA TGG CAT GCA CAA AAA
*hla*_R	TAT CAG TTG GGC TCT CTA AAA
*icaA*_F	CGC ACT CAA AGG CAT T
*icaA*_R	CCA GCA AGT GTC TGA CTT CG
*rot*_F	TCG CTT TCA ATC TCG CTG AA
*rot*_R	CGA CAC TGT ATT TGG AAT TTT GCA
*saeS*_F	AAT CCA GAA CCA CCC GTT TT
*saeS*_R	ACG CCA CTT GAG CGT ATT TT
*sarA*_F	GCA CAA CAA CGT AAA AAA ATC GAA
*sarA*_R	TTC GTT GTT TGC TTC AGT GAT TC
*sod*_F	CCA ATG TAG TCA GGG CGT TT
*sod*_R	GTT CAG GTT GGG CTT GGT TA

Biolabs) was followed by end repair, 5′ phosphorylation, and dA-tailing. Libraries were sequenced on a partial lane of Illumina HiSeq 4000 with 150 bp paired-end sequencing. Quality of sequence data was assessed using FastQC. All reads were quality filtered and trimmed using Trimmomatic version 0.36 with default settings (40). Reads were mapped to *Staphylococcus aureus* subsp. *aureus* USA300_FPR3757 genome using Bowtie2 version 2.2.6 (41), and hit count for individual genes was generated using the featurecounts command in the Rsubread package version 1.5.2 (42). Genes with fewer than 10 reads were dropped from the analysis for differential expression. Differential expression for each gene was assessed using Wald tests implemented in DESeq2 (43). Genes with an adjusted *P* value of <0.05 and absolute $\log_2$(FC) of >1 were categorized as differentially expressed genes.

GO enrichment analyses were conducted using the *goseq* version 1.42.0 package in R (44). Gene ontology (GO) terms and gene lengths were extracted for each gene in the *Staphylococcus aureus* subsp. *aureus* USA300_FPR3757 from the UniProt website (45). We determined whether DEGs between treatments were significantly overrepresented within molecular function, biological process, and cellular component GO terms using a Wallenius approximation and accounting for gene length bias using a probability weight function. Because of the inherent difficulties with multiple testing and correcting for multiple testing in GO analyses, we simply consider any term with *P* of <0.01 statistically significant. KEGG pathway enrichment analyses were conducted using the KEGGREST Bioconductor package version 1.30.1 (46) and a custom script (available upon request). KEGGREST was used to download lists of pathways and genes within pathways from the KEGG website for *Staphylococcus aureus* subsp. *aureus* USA300_FPR3757 (organism code *saa*). We assessed whether DEGs are overrepresented in certain pathways by using a Wilcoxon rank-sum test to determine whether adjusted *P* values for differential expression of genes within a focal pathway are lower than the adjusted *P* values for differential expression of genes that are not within the pathway.

Data availability. The raw Illumina reads have been deposited in NCBI's BioProject database under accession number PRJNA715655.

SUPPLEMENTAL MATERIAL

Supplemental material is available online only.

SUPPLEMENTAL FILE 1, PDF file, 0.6 MB.

SUPPLEMENTAL FILE 2, XLSX file, 0.4 MB.

ACKNOWLEDGMENTS

We thank members of the Kulkarni lab for scientific discussions and comments during the course of this project and the writing of this manuscript.

This work was supported by the Louisiana Board of Regents award LEQSF(2017-20)-RD-A-21 (to R.K.), the University of Louisiana at Lafayette, Dean's Startup Fund (to R.K.), the UL Lafayette Undergraduate research mini grant (to R.K.), and the National Science Foundation award OIA-1920858 (to N.J.K.).

REFERENCES

1. Medina M, Castillo-Pino E. 2019. An introduction to the epidemiology and burden of urinary tract infections. Ther Adv Urol 11:1756287219832172. https://doi.org/10.1177/1756287219832172.
2. Bishara J, Goldberg E, Leibovici L, Samra Z, Shaked H, Mansur N, Paul M. 2012. Healthcare-associated vs. hospital-acquired Staphylococcus aureus bacteremia. Int J Infect Dis 16:e457–e463. https://doi.org/10.1016/j.ijid.2012.02.009.
3. Stokes W, Parkins MD, Parfitt ECT, Ruiz JC, Mugford G, Gregson DB. 2019. Incidence and outcomes of Staphylococcus aureus bacteriuria: a population-based study. Clin Infect Dis 69:963–969. https://doi.org/10.1093/cid/ciy1000.
4. Muder RR, Brennen C, Rihs JD, Wagener MM, Obman A, Stout JE, Yu VL. 2006. Isolation of Staphylococcus aureus from the urinary tract: association of isolation with symptomatic urinary tract infection and subsequent staphylococcal bacteremia. Clin Infect Dis 42:46–50. https://doi.org/10.1086/498518.
5. Karakonstantis S, Kalemaki D. 2018. Evaluation and management of Staphylococcus aureus bacteriuria: an updated review. Infection 46:293–301. https://doi.org/10.1007/s15010-017-1100-6.
6. Gad GF, El-Feky MA, El-Rehewy MS, Hassan MA, Abolella H, El-Baky RM. 2009. Detection of icaA, icaD genes and biofilm production by Staphylococcus aureus and Staphylococcus epidermidis isolated from urinary tract catheterized patients. J Infect Dev Ctries 3:342–351. https://doi.org/10.3855/jidc.241.
7. Remy L, Carriere M, Derre-Bobillot A, Martini C, Sanguinetti M, Borezee-Durant E. 2013. The Staphylococcus aureus Opp1 ABC transporter imports nickel and cobalt in zinc-depleted conditions and contributes to virulence. Mol Microbiol 87:730–743. https://doi.org/10.1111/mmi.12126.
8. Hiron A, Posteraro B, Carriere M, Remy L, Delporte C, La Sorda M, Sanguinetti M, Juillard V, Borezee-Durant E. 2010. A nickel ABC-transporter of Staphylococcus aureus is involved in urinary tract infection. Mol Microbiol 77:1246–1260. https://doi.org/10.1111/j.1365-2958.2010.07287.x.
9. Walker JN, Flores-Mireles AL, Pinkner CL, Schreiber HLt, Joens MS, Park AM, Potretzke AM, Bauman TM, Pinkner JS, Fitzpatrick JAJ, Desai A, Caparon MG, Hultgren SJ. 2017. Catheterization alters bladder ecology to potentiate Staphylococcus aureus infection of the urinary tract. Proc Natl Acad Sci U S A 114:E8721–E8730. https://doi.org/10.1073/pnas.1707572114.
10. Carrel M, Perencevich EN, David MZ. 2015. USA300 methicillin-resistant Staphylococcus aureus, United States, 2000-2013. Emerg Infect Dis 21:1973–1980. https://doi.org/10.3201/eid2111.150452.
11. John PP, Baker BC, Paudel S, Nassour L, Cagle H, Kulkarni R. 2020. Exposure to moderate glycosuria induces virulence of group B streptococcus. J Infect Dis https://doi.org/10.1093/infdis/jiaa443.
12. Kulkarni R, Antala S, Wang A, Amaral FE, Rampersaud R, Larussa SJ, Planet PJ, Ratner AJ. 2012. Cigarette smoke increases Staphylococcus aureus biofilm formation via oxidative stress. Infect Immun 80:3804–3811. https://doi.org/10.1128/IAI.00689-12.
13. Walker JN, Crosby HA, Spaulding AR, Salgado-Pabon W, Malone CL, Rosenthal CB, Schlievert PM, Boyd JM, Horswill AR. 2013. The Staphylococcus aureus ArlRS two-component system is a novel regulator of agglutination and pathogenesis. PLoS Pathog 9:e1003819. https://doi.org/10.1371/journal.ppat.1003819.
14. Rosenberg M, Gutnick D, Rosenberg E. 1980. Adherence of bacteria to hydrocarbons - a simple method for measuring cell-surface hydrophobicity. FEMS Microbiology Lett 9:29–33. https://doi.org/10.1111/j.1574-6968.1980.tb05599.x.
15. Clarke SR, Mohamed R, Bian L, Routh AF, Kokai-Kun JF, Mond JJ, Tarkowski A, Foster SJ. 2007. The Staphylococcus aureus surface protein IsdA mediates resistance to innate defenses of human skin. Cell Host Microbe 1:199–212. https://doi.org/10.1016/j.chom.2007.04.005.
16. Otto M. 2013. Community-associated MRSA: what makes them special? Int J Med Microbiol 303:324–330. https://doi.org/10.1016/j.ijmm.2013.02.007.
17. Lopez R, Ronda-Lain C, Tapia A, Waks SB, Tomasz A. 1976. Suppression of the lytic and bactericidal effects of cell wallinhibitory antibiotics. Antimicrob Agents Chemother 10:697–706. https://doi.org/10.1128/AAC.10.4.697.
18. Brooks T, Keevil CW. 1997. A simple artificial urine for the growth of urinary pathogens. Lett Appl Microbiol 24:203–206. https://doi.org/10.1046/j.1472-765x.1997.00378.x.
19. Bouatra S, Aziat F, Mandal R, Guo AC, Wilson MR, Knox C, Bjorndahl TC, Krishnamurthy R, Saleem F, Liu P, Dame ZT, Poelzer J, Huynh J, Yallou FS, Psychogios N, Dong E, Bogumil R, Roehring C, Wishart DS. 2013. The human urine metabolome. PLoS One 8:e73076. https://doi.org/10.1371/journal.pone.0073076.
20. Stauff DL, Skaar EP. 2009. The heme sensor system of Staphylococcus aureus. Contrib Microbiol 16:120–135. https://doi.org/10.1159/000219376.
21. Hammer ND, Skaar EP. 2011. Molecular mechanisms of Staphylococcus aureus iron acquisition. Annu Rev Microbiol 65:129–147. https://doi.org/10.1146/annurev-micro-090110-102851.
22. Roos V, Ulett GC, Schembri MA, Klemm P. 2006. The asymptomatic bacteriuria Escherichia coli strain 83972 outcompetes uropathogenic E. coli strains in human urine. Infect Immun 74:615–624. https://doi.org/10.1128/IAI.74.1.615-624.2006.
23. Ipe DS, Ben Zakour NL, Sullivan MJ, Beatson SA, Ulett KB, Benjamin WH, Jr, Davies MR, Dando SJ, King NP, Cripps AW, Schembri MA, Dougan G, Ulett GC. 2016. Discovery and characterization of human-urine utilization by asymptomatic-bacteriuria-causing Streptococcus agalactiae. Infect Immun 84:307–319. https://doi.org/10.1128/IAI.00938-15.
24. Berube BJ, Bubeck Wardenburg J. 2013. Staphylococcus aureus alpha-toxin: nearly a century of intrigue. Toxins (Basel) 5:1140–1166. https://doi.org/10.3390/toxins5061140.
25. von Eiff C, Friedrich AW, Peters G, Becker K. 2004. Prevalence of genes encoding for members of the staphylococcal leukotoxin family among clinical isolates of Staphylococcus aureus. Diagn Microbiol Infect Dis 49:157–162. https://doi.org/10.1016/j.diagmicrobio.2004.03.009.
26. Jenkins A, Diep BA, Mai TT, Vo NH, Warrener P, Suzich J, Stover CK, Sellman BR. 2015. Differential expression and roles of Staphylococcus aureus virulence determinants during colonization and disease. mBio 6:e02272-14. https://doi.org/10.1128/mBio.02272-14.
27. Supersac G, Piemont Y, Kubina M, Prevost G, Foster TJ. 1998. Assessment of the role of gamma-toxin in experimental endophthalmitis using a hlg-deficient mutant of Staphylococcus aureus. Microb Pathog 24:241–251. https://doi.org/10.1006/mpat.1997.0192.
28. Malachowa N, Whitney AR, Kobayashi SD, Sturdevant DE, Kennedy AD, Braughton KR, Shabb DW, Diep BA, Chambers HF, Otto M, DeLeo FR. 2011. Global changes in Staphylococcus aureus gene expression in human blood. PLoS One 6:e18617. https://doi.org/10.1371/journal.pone.0018617.
29. Nilsson IM, Hartford O, Foster T, Tarkowski A. 1999. Alpha-toxin and gamma-toxin jointly promote Staphylococcus aureus virulence in murine septic arthritis. Infect Immun 67:1045–1049. https://doi.org/10.1128/IAI.67.3.1045-1049.1999.
30. Parker D, Prince A. 2012. Immunopathogenesis of Staphylococcus aureus pulmonary infection. Semin Immunopathol 34:281–297. https://doi.org/10.1007/s00281-011-0291-7.
31. Ponnuraj K, Bowden MG, Davis S, Gurusiddappa S, Moore D, Choe D, Xu Y, Hook M, Narayana SV. 2003. A "dock, lock, and latch" structural model for a staphylococcal adhesin binding to fibrinogen. Cell 115:217–228. https://doi.org/10.1016/s0092-8674(03)00809-2.
32. Flores-Mireles AL, Walker JN, Potretzke A, Schreiber HLt, Pinkner JS, Bauman TM, Park AM, Desai A, Hultgren SJ, Caparon MG. 2016. Antibody-based therapy for enterococcal catheter-associated urinary tract infections. mBio 7(5):e01653-16. https://doi.org/10.1128/mBio.01653-16.

33. Cardile AP, Sanchez CJ, Samberg ME, Romano DR, Hardy SK, Wenke JC, Murray CK, Akers KS. 2014. Human plasma enhances the expression of Staphylococcal microbial surface components recognizing adhesive matrix molecules promoting biofilm formation and increases antimicrobial tolerance In Vitro. BMC Res Notes 7:457. https://doi.org/10.1186/1756-0500-7-457.
34. Krismer B, Liebeke M, Janek D, Nega M, Rautenberg M, Hornig G, Unger C, Weidenmaier C, Lalk M, Peschel A. 2014. Nutrient limitation governs Staphylococcus aureus metabolism and niche adaptation in the human nose. PLoS Pathog 10:e1003862. https://doi.org/10.1371/journal.ppat.1003862.
35. Alteri CJ, Smith SN, Mobley HL. 2009. Fitness of Escherichia coli during urinary tract infection requires gluconeogenesis and the TCA cycle. PLoS Pathog 5:e1000448. https://doi.org/10.1371/journal.ppat.1000448.
36. Tenover FC, Goering RV. 2009. Methicillin-resistant Staphylococcus aureus strain USA300: origin and epidemiology. J Antimicrob Chemother 64:441–446. https://doi.org/10.1093/jac/dkp241.
37. Bagale K, Paudel S, Cagle H, Sigel E, Kulkarni R. 2020. Electronic cigarette (e-cigarette) vapor exposure alters the streptococcus pneumoniae transcriptome in a nicotine-dependent manner without affecting pneumococcal virulence. Appl Environ Microbiol 86:e02125-19. https://doi.org/10.1128/AEM.02125-19.
38. Lather P, Mohanty AK, Jha P, Garsa AK. 2016. Contribution of cell surface hydrophobicity in the resistance of Staphylococcus aureus against antimicrobial agents. Biochem Res Int 2016:1091290. https://doi.org/10.1155/2016/1091290.
39. Peignier A, Planet PJ, Parker D. 2020. Differential induction of type i and iii interferons by Staphylococcus aureus. Infect Immun 88:e00352-20. https://doi.org/10.1128/IAI.00352-20.
40. Bolger AM, Lohse M, Usadel B. 2014. Trimmomatic: a flexible trimmer for Illumina sequence data. Bioinformatics 30:2114–2120. https://doi.org/10.1093/bioinformatics/btu170.
41. Langmead B, Salzberg SL. 2012. Fast gapped-read alignment with Bowtie 2. Nat Methods 9:357–359. https://doi.org/10.1038/nmeth.1923.
42. Liao Y, Smyth GK, Shi W. 2019. The R package Rsubread is easier, faster, cheaper and better for alignment and quantification of RNA sequencing reads. Nucleic Acids Res 47:e47. https://doi.org/10.1093/nar/gkz114.
43. Love MI, Huber W, Anders S. 2014. Moderated estimation of fold change and dispersion for RNA-seq data with DESeq2. Genome Biol 15:550. https://doi.org/10.1186/s13059-014-0550-8.
44. Young MD, Wakefield MJ, Smyth GK, Oshlack A. 2010. Gene ontology analysis for RNA-seq: accounting for selection bias. Genome Biol 11:R14. https://doi.org/10.1186/gb-2010-11-2-r14.
45. UniProt C. 2019. UniProt: a worldwide hub of protein knowledge. Nucleic Acids Res 47:D506–D515.
46. Tenenbaum D. 2019 KEGGREST: client-side REST access to KEGG. R package version 1.26.1.